VALIDATION OF THE ESTIMATION OF CORNEAL ABERRATIONS FROM VIDEOKERATOGRAPHY: A TEST ON KERATOCONUS EYES.

S. Barbero, BSc. S. Marcos, Ph.D. J. Merayo-Lloves, M.D., Ph.D. E. Moreno-Barriuso, Ph.D.

From Instituto de Óptica, Consejo Superior de Investigaciones Científicas, Madrid, Spain (Barbero, Marcos, Moreno-Barriuso), Instituto de Oftalmobiología Aplicada, Universidad de Valladolid, Spain (Merayo-Lloves). CSIC and Carl Zeiss, Spain sponsored a research fellowship for Mr. Barbero. Ministerio de Educación y Cultura, Spain, provided a research fellowship to Dr. Moreno-Barriuso. This research was funded by grants TIC98-0925-C02-01 (Ministerio de Educación y Cultura, Spain) and CAM: 08.7/0010/2000 (Comunidad Autónoma de Madrid, Spain). Carl Zeiss, Spain lent a Mastervue Atlas Corneal Topography System. The authors have no proprietary interest in the materials presented in this article. The authors wish to acknowledge Ms Lourdes Llorente for her help with data collection and analysis, and Mr Raúl Martín for his contributions in the early stages of the study.
Correspondence: Sergio Barbero. Instituto de Óptica, Consejo Superior de Investigaciones Científicas, Serrano 121, 28006, Madrid, Spain. Fax: 34-915645557. Tlf: 34-915616800. Email: iodb324@io.cfmac.csic.es.

PURPOSE: To validate the estimation of corneal aberrations from videokeratography against a laser ray tracing technique (LRT) that measures total eye aberrations, in eyes with cornea-dominated wave aberrations (i.e. keratoconus).
METHODS: We measured total and corneal wave aberrations of 3 eyes diagnosed with keratoconus by slit-lamp microscope examination and corneal topography: two eyes from one patient (A) with early keratoconus and one eye with a more advanced keratoconus (B). Total aberrations were measured with LRT. Corneal aberrations were obtained from corneal elevation data measured with a Humphrey Instruments corneal videokeratoscope, and using custom software that performs a virtual a ray tracing on the measured front corneal surface. RESULTS: 1) The keratoconus eyes show a dramatic increase in aberrations (both corneal and total) particularly coma-like terms respect of a group of normal eyes (3.74 times higher on average). 2) Anterior corneal surface aberrations and total aberrations are very similar in keratoconus. 3) This similarity is greater for patient A, suggesting a possible implication of the posterior corneal surface in patient B. CONCLUSIONS 1) The similarity found between corneal and total aberration patterns in keratoconus provides a cross-validation of both types of measurements (corneal topography and aberrometry 2) Both techniques are useful in diagnosing and quantifying optical degradation imposed by keratoconus.

While the presence of optical imperfections in the eye beyond conventional refractive errors (known as optical aberrations) have been noticed for more than a century[1], it is only in the last few years when they have been considered from a clinical perspective. The interest has been mainly drawn by the evaluation of refractive surgery outcomes, and by the increasing possibilities of correcting (through surgery or other means) these high order errors[2,3,4]. Corneal topography systems are widely used in the clinic, and in particular, corneal aberrations have been measured following refractive surgery, and the results have been correlated to visual performance[5,6]. However, the optical quality of the human eye is determined by the optical properties of both the cornea and the lens, as well as to their relative alignment and to the position of the pupil[7]. For this reason the measurement of the total aberrations provides the most complete description of the image forming properties of the eye. Several types of aberrometers have been used to assess the ocular aberrations in normal eyes[8,9,10] and following refractive surgery[11,12,13]. Undoubtedly, the combination of the information provided by corneal topography and aberrometry provides interesting insight into the properties of the individual ocular components[14,15]. However, both techniques rely on very different principles. Typical corneal topographers project a Placido disk (a set of concentric rings) onto the anterior surface of the cornea. Corneal elevation maps are obtained from the distortions of the reflected rings[16]. The aberrations caused by the front surface of the cornea are then computed by theoretical ray tracing[17,18]. However, typical aberrometers measure the deviations of beams projected onto the retina through different pupil locations (i.e. laser ray tracing[19], spatially resolved refractometer[10] or Tscherning´s aberroscope[20]), or analyze the wavefront as it emerges out of the eye (i.e. Hartmann-Shack[9]). Factors affecting resolution and accuracy are very different across methods (videokeratography and aberrometry). Whereas the wave aberration is computed directly from a set of ray aberrations, the corneal heights are computed from the ring positions and surface location measured from the video images[16].

Total aberrations are measured directly, whereas some assumptions (i.e. index of refraction) are needed to compute corneal aberrations. Prior to comparing total and corneal aberrations, it seems necessary to prove that both techniques are directly comparable. The ideal test are eyes where total and corneal aberrations should be identical, or at least eyes where total aberrations are dominated by the aberrations of the front surface of the cornea. An approximate model of the first case is an aphakic eye. An approximate model of the second is a keratoconus. Given the distinct nature of the two cases, we will treat them separately. In the current paper, we will study the keratoconus case.

The front surface of the cornea is the major refractive component in the eye, and it is strongly distorted in eyes suffering from keratoconus[21,22]. Important similarities are therefore to be expected between anterior corneal aberration and total aberration patterns. Furthermore, this comparison can be a good cross-validation of the two techniques used in this study: 1) Computation of anterior corneal aberrations by simulated ray tracing on corneal elevation maps as measured by a Humphrey Atlas corneal videokeratoscope, and 2) Laser Ray Tracing measurements of ocular aberrations. Although presumably relatively small in conventional keratoconus, the crystalline lens and posterior corneal surface play a role in overall image quality[14,23]. This indicates that the measurement of total aberrations may have advantages over the measurement of just anterior corneal aberrations, allowing a better comparison with visual performance. For example, posterior keratoconus, characterized by a conical protrusion of the posterior corneal curvature, a thinned stroma and non-protruding anterior surface[24], could be detected measuring the total aberrations, while anterior aberrations would appear as normal. A lack of correspondence between total and anterior corneal aberrations in a diagnosed keratoconus may well be indicative of an involvement of the posterior corneal surface.

PATIENTS AND METHODS

Total and corneal aberrations were measured on three eyes from two patients: both eyes of patient A (female, aged 34) and right eye of patient B (female, age 40). The three eyes were diagnosed with keratoconus by slit-lamp microscope examination, corneal topography, presence of high astigmatism, and reduced visual acuity, being in an early stage for patient A and more advanced in patient B. Computer-assisted videokeratography (Humphrey-Zeiss Mastervue Atlas Corneal Topography system) was performed during the experimental sessions. Figure 1 shows topographic power maps, revealing corneal inferior steepening in all eyes within ranges reported in the literature as indicative of keratoconus[21,25,26].

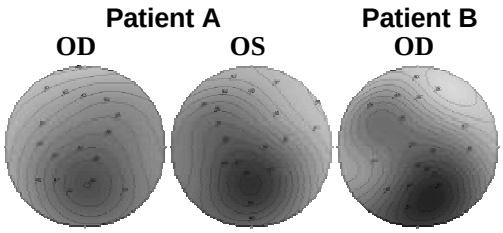

Figure 1 shows topographic power maps, revealing corneal inferior steepening in all eyes within ranges reported in the literature as indicative of keratoconus[21,25,26]

Patient A's autorefractometer refraction was –2.5D –2.5D x 35º (OD) and –2D –2D x 125º (OS). Best spectacle-corrected visual acuity (BSCVA) was 20/50 and 20/40 respectively. Patient B's refraction was –5.25D –5.25D x 33º (OD), with a BSCVA of 20/100. The two types of measurements (corneal and total aberrations) were performed in the same experimental session, after recent clinical screening. Pupils were dilated with one drop of tropicamide 1%. The patients signed informed consent forms approved by institutional ethical committees.

Total aberrations were measured using a Laser Ray Tracing (LRT) Technique. This method has been described in detail elsewhere[3,4]. In brief, a set of 37 parallel laser pencils (543 nm HeNe laser) sample the pupil sequentially following a hexagonal pattern. A full scan takes ~4 sec. This technique has been shown to provide similar results and variability than other techniques such as Shack-Hartman and Spatially Resolved Refractometer[27]. Simultaneously, the corresponding retinal images are projected onto a high-resolution CCD camera. Figure 2 (a) shows the set of retinal images for one of the runs recorded in a keratoconus eye (Patient A, OD). The location indicates the corresponding entry pupil position. Measurements were done over a 6.51

mm effective pupil diameter for patient A (step-size= 1-mm) and 5.5 mm for patient B (step-size=0.8-mm). We had to reduce slightly the sampled area due to the large amount of aberrations present in patient B. Even with best spherical and cylindrical correction, the aerial images for the most eccentric locations of 6.51 mm pupil did not fit in the CCD array. Figure 2 (b) shows a joint plot of the centroids of those images (spot diagram). The deviation of each centroid from the principal ray (or centroid of the retinal image of the ray passing through the pupil center) is proportional to derivate (slope) of the wave aberration at the corresponding pupil location. This set of values was fitted to the derivatives of a 7th order Zernike expansion (35 Zernike coefficients). A session consisted of five runs (37 images each). All the measurements were foveal. The pupil was continuously monitored with an IR system, and the subjects were stabilized by means of a forehead rest and dental impression, to ensure proper centration and to facilitate positioning reproducibility.

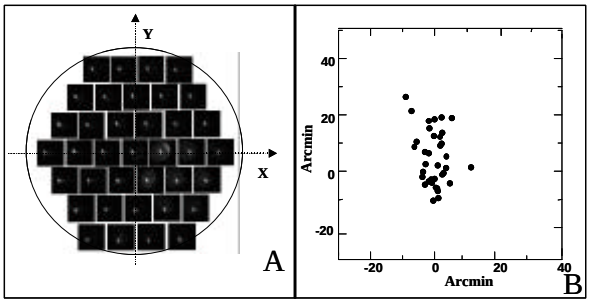

Figure 2. .A) Set of retinal images, captured by the high resolution CCD in Laser Ray Tracing as a function of entry pupil location, for patient A, OS. Each retinal aerial image is located at the corresponding entry pupil location. Pupil effective diameter was 6.51 mm. **B)** Spot diagram, i.e. joint plot of centroids of the retinal images shown in A.

Corneal elevation maps were obtained from each eye, using the Mastervue Corneal Topography System (Humphrey Instruments, San Leandro, CA). Except for initial control experiments, only one map was captured per eye. The patient fixated foveally, and stabilization was achieved by chin and forehead rests. The output text files included axial and radial positions, height and curvature data, all obtained from videokeratography images by an arc step reconstruction method[16]. These data were processed in Matlab (Mathworks, Natik, MA). Points outside a 10-mm region were rejected, since they were usually covered by eyelids or subject to distortion. Polar coordinates were transformed into cartesian coordinates, and the data were interpolated to achieve a regular sampling. The corneal height surface was fit to a 7th order Zernike polynomial expansion[28]. Figure 3 (a) shows a typical corneal elevation map in a keratoconic eye (Patient A, OS). In order to show the irregularities, we have subtracted the first six terms of Zernike polynomial fit to the height data from the raw height data[29]. First derivatives in *x* and *y*, and second cross derivatives in *xy* from corneal fitted surface were also computed. These data are the input for the optical design program, Zemax V.9 (Focus Software, Tucson, AZ), used to perform a virtual ray tracing simulation. We simulated a set of parallel light pencils (λ=543nm) coming from infinity, sampling 64 x 64 points of the corneal surface (in a rectangular grid). The indices of refraction were taken as that of the air and the aqueous humor (1.3391). Figure 3(b) shows the simulated spot diagram for the example shown in Figure 3(a).

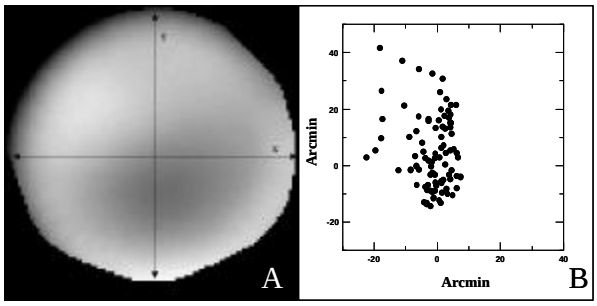

Figure 3. A): Residual height map of patient A, OS. A Zernike polynomial fitting (up to the 2nd order) has been substracted from raw height data, in order to enhance relevant features[29]. **B)** Spot diagram obtained by virtual ray tracing on corneal height data (Patient A, OS). Stop pupil diameter was 6.51 mm after appropriate centration.

The corneal wave aberration was described as a 7th order Zernike polynomial expansion and evaluated at the plane of best focus. Unlike the LRT measurements (where the reference was the pupil center), corneal topography typically uses the corneal reflex for alignment. The system does not allow the acquisition of out-of-focus images, so images with centration errors of more than about 0.25 mm were not captured. Proper alignment of corneal and total wave aberration is necessary for direct comparison[30]. To compensate for possible shifts in the reference axis, we developed custom software to locate the pupil position that produced minimum difference of corneal to total aberrations. Corneal aberrations were computed

over a large pupil diameter (10 mm) and re-computed over a smaller pupil (matching the pupil size of total aberration measurements), moving the center over a 1-mm square region around the position of the corneal reflex, at 0.1-mm steps. A difference total-corneal map was computed for each pupil location. This surface showed a minimum, typically slightly decentered from the corneal reflex. Independent observations of the corneal reflex relative to the pupil center[31] performed on control subjects show that this procedure identifies well the pupil center (inaccessible otherwise from the corneal topography images).

Even if the decentration between the corneal reflex and pupil center are corrected, there is still a tilt between the keratometric axis, used in videokeratography, and the line of sight, used in laser ray tracing. This angle can be computed from: the distance between the corneal intersect of the keratometric axis and corneal sighting center (intersection of line of sight with anterior corneal surface) and the distance from the fixation point to front corneal surface, 148.3 mm in our videokeratoscope (Steve Kaatmann, Zeiss Humphrey Systems. Personal communication).As the position of corneal sighting center is not available in our patients, we assumed the average value reported by Mandell et al[32] (0.38±0.10 mm, across 20 normal eyes). With these values we computed a corneal tilt of ~ 0.15 deg, which we neglected in further computations. For patient B eye we found that, considering this average tilt, RMS changes only by 2.6% (aphakic eye) for 3rd order terms, and 0.6 % for spherical aberration.

We analyzed individual Zernike terms to compare the corneal and total aberrations. Root-mean-square wavefront error (RMS) was used as an optical quality metric

RESULTS

Figure 4 shows total (upper row) and corneal (lower row) wave aberration maps for patients A (OD and OS) and B (OD). Contours have been plotted at 1- m intervals. Pupil sizes are 6.51-mm for patient A and 5.5-mm for patient B. The gray scale for corneal and total aberrations is the same for each patient. Tilt and defocus have been cancelled in all eyes.

There is a good correspondence between corneal and total wavefront maps. Peak-to-valley values are double in patient B than in patient A.

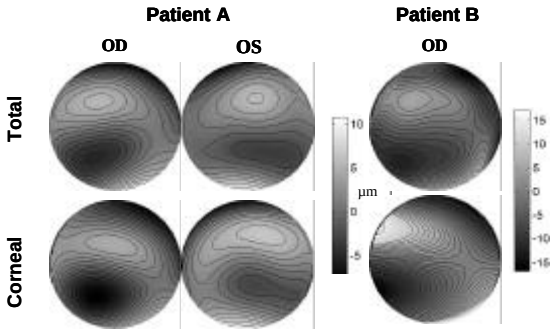

Figure 4. Wave aberration patterns (without tilts and defocus) in the 3 measured eyes, for total aberrations (upper row) and corneal aberration (lower row). Contour lines are plotted every 1 μm. The gray scale pattern represent wave aberration heights in microns. Diameters were 6.51 mm in patient A and 5.51mm in patient B.

Figure 5 compares corneal (open diamonds) and total (solid circles) Zernike coefficients for each eye, following the ordering and notation recommended by the Optical Society of America Standard Committee[33]. For patient A, there is a good correspondence between total and corneal aberrations. In both eyes of this subject, the dominant aberration is the coma term Z_3^{-1}, which is higher than astigmatism. The dominance of coma is also evident in the wave aberration plots.

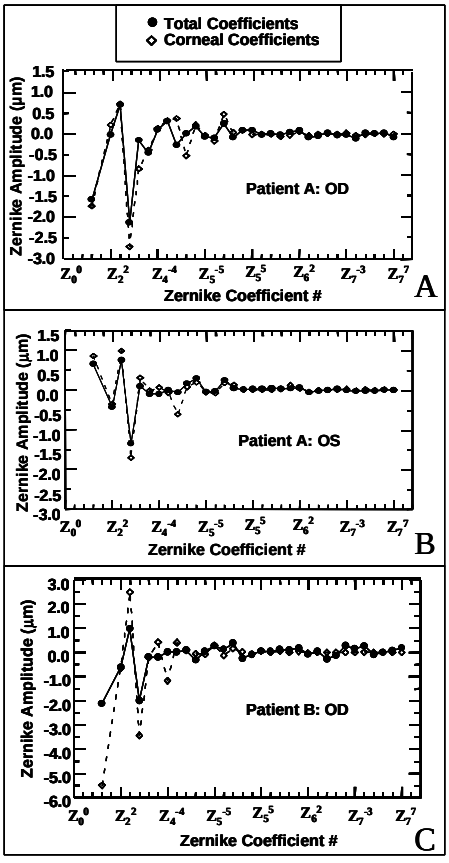

Figure 5. Total (solid circles) and corneal (empty diamonds) aberrations for Patient A, OD (A), Patient A, OS (B) and Patient

B, OD (C). Notation follows the OSA Standard Committee's recommendations[33].

The largest difference between total and corneal aberration for patient A was found for spherical aberration (coefficient of Z_4^0 element). For the right eye, corneal and total spherical aberration have different sign and show a total difference of 0.74 m, whereas for the left eye corneal spherical aberration exceeds total spherical aberration by 0.55 m. This indicates a compensation of corneal spherical aberration by spherical aberration of the crystalline lens. This balance of spherical aberration is a common finding in normal eyes[14,34,35]. While the progressive disease seems to affect high order terms (particularly coma) of both corneal and total aberrations, it does not seem to modify the amount of spherical aberration (Z_4^0).

In patient B, the correspondence between corneal and total Zernike terms is worse than for patient A. Some exceptional terms show large differences. Major differences are found in astigmatic term Z_2^{-2} (4.58 m difference), third order term Z_3^3 (0.63 mm) and 4th order term Z_4^{-4} (1.15 m). In this subject, astigmatism is the dominant term, followed by coma.

For the sake of clarity, error bars have not been plotted in Figure 5. Control experiments performed in one patient show a mean standard deviation of 0.08 m for the corneal Zernike coefficients (averaged across terms, excluding tilts and defocus). The mean standard deviation for the total Zernike coefficients (averaging across the three eyes and coefficients) was 0.13 m.

Table 1 shows the RMS for different terms and orders evaluated for the three eyes. There is a clear predominance of 3rd order (coma-like) terms, both in corneal and total aberration. In terms of variance (squared RMS), they represent 61% (70.72% for patient A and 41.53% for patient B) of the aberration (excluding tilt and defocus, but including astigmatism). Excluding astigmatism, coma-like terms represent 90.85% of the variance. Mean 3rd order aberration (2.02±0.41) in this group of keratoconus eyes exceeds by a factor of 3.74 the average 3rd order aberration (0.54±0.30) of a group of normal eyes. This control group of 22 eyes from 12 subjects was within similar age range (28±5 years) and within similar refractive errors (-6.42±2.5 D sphere)[11].

Table 1. RMS and Zernike corneal and total terms.

	PatientA OD		PatientA OS		PatientB OD	
	Total	Corneal	Total	Corneal	Total	Corneal
Z_2^{-2}	1.58	1.73	-0.64	-0.85	-2.1	-5.24
Z_2^{+2}	0.01	-0.22	0.44	0.34	-0.6	-0.66
RMS 2rd to 7rd order (except defocus)	2.84	3.55	1.8	2.3	3.25	7.1
RMS 3 order	2.29	2.95	1.55	1.99	2.23	4.26
RMS 3rd & higher orders	2.36	3.09	1.62	2.11	2.4	4.46
RMS 4 order	0.46	0.77	0.35	0.66	0.33	1.24
RMS 5rd & higher orders	0.38	0.52	0.28	0.27	0.82	0.38
$\frac{\text{Variance } 3^{rd}*100}{\text{Var. } 2^{rd} \text{ \& higher (no defocus)}}$	64.9	69.1	74.1	74.9	47.1	36
$\frac{\text{Variance } 3^{rd}*100}{\text{Variance } 3^{rd} \text{ \& higher}}$	94.1	91.1	91.6	89	86.3	93

DISCUSSION

Corneal and total aberrations were estimated in three eyes, all diagnosed with keratoconus at different stages of the disease. We found good correspondence between corneal and total aberrations, particularly in both eyes of patient A, indicating that the overall aberration pattern is dominated by the front corneal surface, and that both methods are able to capture similarly the distortions produced by the irregular cornea. Our results show that Humphrey Mastervue Atlas corneal topography system and laser ray tracing are both adequate tools to analyze optical quality in keratoconus. As reported previously[36] image degradation in keratoconus is mainly due to an increase in higher order aberrations, particularly coma. In the three affected eyes from this study, third order aberrations increase by a factor of 4.24, 2.87 & 4.13 respectively with respect to normal eyes[11].

We have shown both techniques provided good results (valid topography data and good quality retinal images in LRT) in these eyes with abnormally high order aberrations. Both techniques failed in two eyes with a highly advanced stage of keratoconus (one patient scheduled for keratoplasty, not shown here). In these eyes, the videokeratographic images were so distorted that the commercial software did not accept the data. Many of the LRT aerial retinal images were highly diffused (probably due to corneal scarring), and even after compensation of spherical error they did not fit within the CCD area. There are many differences inherent to the techniques under use, and nevertheless the similarity of the corneal and total aberration pattern is high, at least for patient A. The accuracy of the measurements is determined by different

factors. The fact that despite these differences the results are similar indicate that these factors do not seem to be essential. Studies of the accuracy of corneal topography devices show that they can measure to a root-mean-square error of 3.7±0.7 μm, at least regular surfaces (5.4-mm radius aspheric surfaces)[37]. It may be argued that errors may arise from smooth Zernike fitting to the corneal heights. To test the limitations of the polynomial smoothing of the surface in the patients of this study, we have fitted the corneal heights to Zernike polynomials of increasing order (5^{th} through 10^{th} order) and computed the corresponding root-mean-square fitting errors. We observed that little further improvement is found using expansions of orders higher than 6^{th}. This agrees with previous studies that showed that the optimal number of Zernike terms to fit corneal surface depends on the actual corneal shape, and it is not necessarily the highest order expansion[38]. In this study, we fitted the corneal surface to a 7th order polynomial expansion. For patient A, the root-mean-square fitting error was 0.95 μm and 0.74 μm, for OD and OS respectively. For patient B, the fitting error (3.76 μm) was of the same order than the nominal accuracy of the device. Increasing the Zernike expansion up to the 10^{th} order only reduced this error to 3.52 μm. This finding suggests that this amount of aberrations may set a limit where a Zernike polinomial expansion to the surface can be a good approximation. For patient A, the accuracy of corneal aberrations computation is clearly limited by the topographer, not by the fitting algorithm. To evaluate the influence of topography measurement accuracy on corneal aberrations errors, we simulated a corneal surface with data randomly separated from the original topography data (patient A, left eye) by a mean value of 3.7 μm. We obtained a wavefront average error of 0.005 μm. This wavefront error is lower than run-to-run variability and total wave aberration errors. The Zernike polynomial fit to the 7^{th} order seems to be an appropriate description of wavefront data (both corneal and total). Sampling density in the ray tracing simulation was 4096, but we also tried denser sampling (16384 and 65536) and the differences that we found were negligible. A much sparser sampling (37) was used in LRT experimental measurements of total aberrations, and nevertheless we found consistent results. This suggests that the major aberrations present in keratoconus do not require a dense sampling to be captured.

Our centration algorithm allows direct comparison of corneal and total aberration maps, both centered with respect to the pupil center. Previous studies[32] found a mean distance (in 20 eyes) between corneal sigthing center (pupil center in the cornea) and videokeratography map center of 0.38±0.1 mm. For the eyes shown in this study, we found a mean distance between corneal reflex and pupil center of 0.5±0.1 mm, and 0.6±0.5 mm for a larger population of 89 eyes on which we used the same procedure. This slightly higher differences found in our study could be to the fact that dilated eyes increase pupil center shift by about 0.2 mm on average[39,40].

In summary, we have crossed-validated two techniques for measuring corneal and total aberrations respectively with tests on eyes with keratoconus. They have proved powerful to detect and quantify the aberrations in moderate keratoconus. The data on patient B shown in this paper probably sets a limit where the assumptions of the techniques are valid to provide valid quantitative data. Zernike polinomial corneal height fitting error equals the accuracy of the corneal topography device, and we had to use a smaller pupil diameter in the LRT system in order to capture the entire set of retinal images. Measurements in a very advanced keratoconus failed with both instruments. Finally, part of the differences found between specific terms of corneal and total aberrations in patient B might have been caused by the posterior corneal surface could being affected in advanced keratoconus[22]. In this regard, measurement of overall aberrations has advantages over corneal topography, since it allows capturing possible alterations of the posterior corneal surface. Since they contain information of all optical components (including the crystalline lens) they provide the most complete description of the imaging properties of the eye.

References

1 Helmholtz HV. *Physiological Optics*. J.P.C. Southhall, New York. 1896

2 MacRae SM, Schwiegerling J, Snyder R. Customized corneal ablation and super vision. J Refract Surg 2000;16(suppl):S230-S235.

3 Liang J, Williams D, Miller D. Supernormal vision and high-resolution retinal imaging

through adaptive optics. J Opt Soc Am 1997;14:2884-2892.
4 Navarro R, Moreno E, Bará S, Mancebo T. Phase-plates for wave-aberration compensation in the human eye. Opt Lett 2000;25:236-238.
5 Applegate RA, Howland HC, Sharp RP, Cottingham AJJ, Yee RW. Corneal aberrations and visual performance after radial keratotomy. J Refract Surg 1998;14:397-407.
6 Applegate RA, Hilmantel G, Howland H, Tu EY, Starck T, Zayak J. Corneal first surface optical aberrations and visual performance. J Refract Surg 2000;16:507-514.
7 Marcos S, Burns SA, Prieto PM, Navarro R, Baraibar B. Investigating the sources of monochromatic aberrations and transverse chromatic aberration. Vision Res (In Press) .
8 Navarro R, Losada MA. Aberrations and relative efficiency of light pencils in the living human eye. Optom Vis Sci 1997;74:540-547.
9 Liang J, Grimm B, Golez S, Bille J. Objetive measurement of wave aberrations of the human eye with the use of a Hartmann-Shack wave-front sensor. J Opt Soc Am A 1994;11:1949-1957.
10 He JC, Marcos S, Webb RH, Burns SA. Measurement of the wave-front aberration of the eye by a fast psychophysical procedure. J. Opt. Soc. Am. A. 1998;15:2449-2456.
11 Moreno-Barriuso E, Merayo-Lloves J, Marcos S, Navarro R, Llorente L, Barbero S. Ocular aberrations before and after corneal refractive surgery: LASIK-induced changes measured with Laser Ray Tracing. Invest Ophthalmol Vis Sci 2001;42:1396-1403.
12 Thibos LN, Hong X. Clinical applications of the Shack-Hartmann aberrometer. Optom Vis Sci 1999;76:817-825.
13 Seiler T, Kaemmerer M,Mierdel P, Krinke H-E. Ocular optical aberrations after photorefractive keratectomy for myopia and myopic astigmatism. Arch Ophthalmol 2000;118:17-21.
14 Artal P, Guirao A. Contribution of the cornea and the lens to the aberrations of the human eyes. Opt Lett 1998;23:1713-1715.
15 Marcos S,Barbero S, Llorente L, Merayo-Lloves J. Optical Response to Myopic LASIK Surgery from Total and Corneal Aberration Measurements. Invest Ophthalmol Vis Sci (In press) .
16 Campbell C. Reconstruction of the corneal shape with the MasterVue Corneal Topography System. Optom Vis Sci 1997;74:899-905.
17 Camp JJ, Maguire LJ, Cameron BM, Robb RA. A computer model for the evaluation of the effect of corneal topography on optical performance. Am J Ophthalmol 1990;109:379-386.
18 Sarver EJ,Applegate RA. Modeling and predicting visual outcomes with VOL-3D. J Refract Surg 2000;16:S611-S116.
19 Navarro R, Moreno-Barriuso E. A laser ray tracing method for optical testing. Opt Lett 1999;24:951-953.
20 Mrochen M, Kaemmerer M,Mierdel P, Krinke HE,Seiler T. Principles of Tscherning Aberrometry. J Refract Surgery 2000;16:S570-S571.
21 Maguire LJ,Bourne WM. Corneal topography of early keratoconus. Am J Ophthalmol 1989;108:107-112.
22 Tomidokoro A, Oshika T, Amano S, Higaki S,Maeda N, Miyata K. Changes in anterior and posterior corneal curvatures in keratoconus. Ophthalmology 2000;107:1328.1332.
23 Smith G, Cox MJ, Calver R,Garner LF. The spherical aberration of the crystalline lens of the human eye. Vision Res 2001;41:235-243.
24 Mannis MJ, Lightman J, Plotnik RD. Corneal topography of posterior keratoconus. Cornea 1992;11:351-354.
25 Mohammad H, Hashemi H. A quantitative corneal topography index for detection of keratoconus. J Refract Surg 1998;14:427-436.
26 Maeda N, Klyce SD, Smolek MK, Thompson HW. Automated keratoconus screening with corneal topography analysis. Invest Ophthalmol Vis Sci 1994;35:2749-2757.
27 Moreno-Barriuso E, Marcos S, Navarro R, Burns S. Comparing Laser Ray Tracing, Spatially Resolved Refractometer and Hartmann-Shack Sensor to measure the ocular wave aberration. Optom Vis Sci 2001;78:152-156.
28 Schwiegerling J, Greivenkamp JE,Miller JM. Representation of videokeratoscopic height data with Zernike polynomials. J Opt Soc Am A 1995;12:2105-2113.
29 Schwiegerling J. Cone Dimensions in Keratoconus using Zernike polynomials. Optom Vis Sci 1997;74:963-969.

30 Applegate RA, Thibos LN,Bradley A, Marcos S, Roorda A, Salmon TO, Atchison DA. Reference axis selection: Subcommitte report of the OSA working group to establish standars for measurement and reporting of optical aberrations of the eye. J Refract Surg 2000;16:S656-S658.
31 Marcos S,Burns SA. On the symmetry between eyes of wavefront aberration and cone directionality. Vision Res 2000;40:2437-2447.
32 Mandell RB, Chiang CS,Klein SA. Location of the major corneal reference points. Optom Vis Sci. 1995;72:776-784.
33 Thibos LN, Applegate RA, Schwiegerling JT, Webb R, Members VST. Standars for reporting the optical aberrations of eyes. Vision Science and its Applications. Tops Volume 2000;35.
34 El Hage SG, Berny F. Contribution of the crystalline lens to the spherical aberration of the eye. Journal of the Optical Society of America 1973;63:205-211.
35 Sivak JG, Kreuzer RO. Spherical aberration of the crystalline lens. Vis.Res. 1983;23:59-70.
36 Lagana MA, Cox IG, Potvin RJ. The effect of keratoconus on the wavefront aberration of the human eye. Invest Ophthalmol Vis Sci (suppl) 2000;41:S679.
37 Schultze RL. Accuracy of corneal elevation with four corneal topography systems. J Refract Surg 1998;14:100-104.
38 Iskander DR, Collins MJ, Davis B. Optimal modeling of corneal surfaces with zernike polynomials. IEEE Trans Biomed Eng 2001;48(1):87-95.
39 Uozato H,Guyton DL. Centering corneal surgical procedures. Am J Ophthalmol 1987;103:264-275.
40 Walsh G. The effect of mydriasis on the pupillary centration of the human eye. Ophthalmic Physiol Opt 1988;8:178-182.